

# The ultimate strength of circular, mild steel plates in uniform compression

Autor(en): **Sherbourne, A.N.**

Objektyp: **Article**

Zeitschrift: **IABSE publications = Mémoires AIPC = IVBH Abhandlungen**

Band (Jahr): **22 (1962)**

PDF erstellt am: **28.05.2024**

Persistenter Link: <https://doi.org/10.5169/seals-18812>

## Nutzungsbedingungen

Die ETH-Bibliothek ist Anbieterin der digitalisierten Zeitschriften. Sie besitzt keine Urheberrechte an den Inhalten der Zeitschriften. Die Rechte liegen in der Regel bei den Herausgebern.

Die auf der Plattform e-periodica veröffentlichten Dokumente stehen für nicht-kommerzielle Zwecke in Lehre und Forschung sowie für die private Nutzung frei zur Verfügung. Einzelne Dateien oder Ausdrucke aus diesem Angebot können zusammen mit diesen Nutzungsbedingungen und den korrekten Herkunftsbezeichnungen weitergegeben werden.

Das Veröffentlichen von Bildern in Print- und Online-Publikationen ist nur mit vorheriger Genehmigung der Rechteinhaber erlaubt. Die systematische Speicherung von Teilen des elektronischen Angebots auf anderen Servern bedarf ebenfalls des schriftlichen Einverständnisses der Rechteinhaber.

## Haftungsausschluss

Alle Angaben erfolgen ohne Gewähr für Vollständigkeit oder Richtigkeit. Es wird keine Haftung übernommen für Schäden durch die Verwendung von Informationen aus diesem Online-Angebot oder durch das Fehlen von Informationen. Dies gilt auch für Inhalte Dritter, die über dieses Angebot zugänglich sind.

# The Ultimate Strength of Circular, Mild Steel Plates in Uniform Compression

*Résistance limite de plaques circulaires en acier doux soumises à des efforts de  
compression uniformes*

*Grenzfestigkeit von Kreisplatten aus normalem Baustahl unter gleichförmigem  
Druck*

A. N. SHERBOURNE

University of Waterloo, Ontario, Canada

## Notation

$m\epsilon_r, m\epsilon_t$	= radial and tangential membrane strains
$b\epsilon_r, b\epsilon_t$	= radial and tangential bending strains
$m\sigma_r, m\sigma_t$	= radial and tangential membrane stresses
$b\sigma_r, b\sigma_t$	= radial and tangential bending stresses
$m_r, m_t$	= radial and tangential bending moments per unit width
$u$	= radial displacement
$\Delta, w$	= deflexion
$r$	= radius
$y, \alpha, \mu, \eta$	= non-dimensional plate radii
$\theta$	= slope
$R$	= plate radius
$z_\mu, z$	= plate depths measured from median surface
$h$	= plate thickness
$\sigma_y$	= yield stress in tension or compression
$\nu$	= Poisson's ratio
$p$	= applied edge stress
$D$	= plate bending stiffness $E h^3/12 (1 - \nu^2)$
$\gamma$	= non-dimensional moment $m/m_p$
$\beta$	= non-dimensional thrust $m\sigma/\sigma_y$
$m_p$	= fully plastic moment per unit width $h^2 \sigma_y/4$

$$\begin{aligned}
 k^2 &= \frac{E}{3\sigma_y(1-\nu^2)} \\
 E &= \text{Modulus of Elasticity} \\
 W, U, x &= \text{functions of } r \\
 s_1 \dots s_4 &= \text{functions of } U, W \text{ and } x \\
 P &= \text{total edge load} \\
 P_y &= \text{"squash" load}
 \end{aligned}$$

### Introduction

FRIEDRICHS and STOKER (1942) discussed the post-buckling behaviour of simply supported circular plates at large deflexion. Their solution was extended to the clamped plate by BODNER (1954). Recently KELLER and REISS (1958) have applied finite difference procedures to describe the bending and buckling of circular plates using a digital computer to obtain numerical results for a wide range of loading and boundary conditions. These investigations have all presupposed unlimited elastic, post-buckling behaviour; in contrast, the present investigation attempts to predict the ultimate strength of circular plates by taking into account plastic behaviour.

The critical load is a wholly elastic concept, being defined as that load at which a bifurcation of equilibrium is possible. In general, a plate will possess an infinite number of critical loads, each load being a solution of the "eigenvalue" problem contingent upon assuming a condition of plane strain throughout the plate; it is only the lowest critical load, however, which is of practical interest. If the loads on a perfectly plane plate are increased slowly, the plate will remain undeformed until the critical load is reached, when it is capable of assuming adjacent bent positions of indifferent equilibrium. In practice, the presence of initial imperfections will cause the plate to deflect at first application of load, the deflexions becoming quite large in the vicinity of the critical load. While a close estimate of the critical load is possible using a Southwell plot, it seems reasonable to regard such a load as an ideal, attainable only when the imperfections in the plate approach zero. When loaded beyond the critical thrust, membrane forces are mobilised and the plate problem reverts to one equilibrium, each load corresponding to a uniquely defined deflexion surface of the plate.

If the transverse deflexions of the plate are small compared with its thickness, it is customary to disregard the mean stresses within the plate which arise from deformations of the median surface due to changes in curvature. This forms the basis of the linear theory for bending and buckling of plates. TIMOSHENKO (1940) has pointed out that this theory leads to considerable discrepancies between prediction and experiment when the deflexions exceed about one half the plate thickness. The linear theory has been known to overestimate the measured stresses in the case of the circular plate bent by terminal

## Elastic-Plastic Behaviour

The graph plots Edge load  $P$  on the vertical axis against Central deflexion  $\omega$  on the horizontal axis. The vertical axis has labels  $P_y$  and  $P_{cr}$ . The horizontal axis has a label  $\omega$  and an origin  $O$ . A solid line, labeled "Mechanism line", starts at  $P_y$  and slopes downwards. A solid curve starts at  $P_{cr}$ , passes through points  $A$ ,  $B$ ,  $C$ , and  $Y$ , and intersects the mechanism line at point  $X$ . Dashed curves  $A'$ ,  $A''$ ,  $C'$ , and  $C''$  are also shown, with points  $X'$  and  $X''$  marked on the mechanism line.

The post-buckling behaviour may be traced in two well defined stages. Stage *AB* is that in which the plate is entirely elastic and it may be shown that the load  $P$  — deflexion  $w$  relationship is of parabola form  $P = P_{cr} + K w^2$  (see Appendix). At point *B* plasticity sets in along the perimeter of the plate. If the plate is simply supported, plasticity occurs in the tangential direction along the support and propagates inward along a set of  $2\pi$  radial hinge lines until, at *C*, a tangential hinge field is developed in the plate. If the plate is clamped around the edge, it is likely that a hinge circle will form at the support before the development of the hinge field in the plate. In theory, it is only



with the formation of a mechanism at  $C$  that the plate is incapable of sustaining additional load and begins to unload. Such unloading alters the nature of the problem from a statical one to one in which dynamic forces should be considered. HOFF (1949) has examined this phenomenon in relation to collapse loads in the stability problem. The present analysis, however, has ignored dynamic effects, regarding the mechanism of unloading as a succession of statical problems leading to a collapse line which has a maximum at the "squash" load of the plate.

The behaviour of real plates differs substantially from that of idealized plates. Real plates possess imperfections which render them liable to deflexions at first application of load. If specific values of the initial imperfection are assumed, the "eigenvalue" problem immediately becomes an equilibrium problem and a unique loading path is defined by  $OA'C'$ . The effect of assuming an increasing imperfection is shown in the path  $OA''C''$ ; the loading path represented by the stability problem is thus a limiting condition of the equilibrium problem when the imperfections in the plate approach zero. It can also be seen that the loading path for real plates will intersect the unloading line in values  $X'$ ,  $X''$ , less than the ideal counterpart  $X$ , the value of the ultimate load being decreased for larger initial imperfections.

The paths represented by  $OA'C'$ ,  $OA''C''$  are those for plates with initial imperfections. If membrane stresses were absent, the loading curve would be a hyperbola asymptotic to the critical load, the deflexions corresponding to each load being a magnification of the imperfections in the ratio  $1/(1 - \frac{P}{P_{cr}})$ . Membrane stresses, however, reduce the deflexions and alter the nature of the load-deflection curve to produce a point of inflexion at the critical load and foster stable equilibrium in the plate in its post-buckling configuration. The present study of the circular plate is restricted to investigating the perfectly plane plate; the resulting collapse load is an upper bound on the behaviour of real plates.

The mechanism line will begin at the "squash" load of the plate since this represents an absolute maximum load which a perfectly plastic plate may sustain. The curve indicates the variation of the applied load with changes in geometry of the plate and may be deduced by considering an arbitrary hinge field and equating the internal and external work for a virtual displacement about an equilibrium position at finite deflexion. The locus so obtained will again furnish an upper bound on the unloading of the plate, the divergence from exact behaviour being a measure of the assumed mechanism. In the present analysis of a simply supported plate a hinge field is assumed based upon a rigid-perfectly plastic stress-strain law. In consequence of the two curves being founded on different stress-strain relationships, the unloading line will intersect the loading path at point  $X$  below  $C$  (Fig. 1). In the case of stocky plates, this discrepancy is negligible since the plates would buckle

near the yield load and the loading path would be characterised by small transverse deflexions before unloading set in. For thin plates, however, the error becomes appreciable since considerable deflexion occurs before the hinge field forms and ultimate load is attained.

### The Loading Path

To obtain the post-buckling loading path for a circular plate in compression, a numerical procedure is developed which obviates the solution of the classical Von Kármán large deflexion equations. In principle, the method follows that suggested by TIMOSHENKO (1940) to describe the behaviour of circular plates bent by edge couples, and HORNE (1956) for determining the elastic-plastic behaviour of struts bent about a principal axis. The method makes use of the equations of equilibrium, moment and thrust and a specified set of initial conditions derived from symmetry at the centre of the plate; it has the powerful advantage of being suitable for programming on a digital computer. Briefly, the procedure may be described as that of choosing numerical values of moment and thrust at the centre of the plate and carrying out a step-by-step integration of the equations of equilibrium to determine the moment and thrust over each interval. The integration is continued to arrive at a critical radius at which the boundary conditions are satisfied. For a simply supported plate the critical radius is that radius at which the radial bending moment vanishes; for the clamped plate, the critical radius is obtained from a condition of zero slope. Having attained the required boundary conditions, it is possible to evaluate boundary tractions and deflexions for the bent plate.

By varying the initial values of moment and thrust at the centre of the plate, several such critical radii can be obtained and contours may be plotted relating the plate size, central deflexion and boundary tractions. For a plate of given size the load-deflexion relationship may be obtained by interpolating between contours of central moment and thrust.

The assumptions and limitations underlying this treatment of the plate problem are listed below:

- a) The thickness is sufficiently small such that shear deformations may be neglected.
- b) Slopes are assumed small to warrant a simplified expression for curvature.
- c) An elastic-perfectly plastic stress-strain relationship is postulated which is identical in tension or compression.
- d) The material is assumed to obey the yield criterion and associated flow rule of Tresca (Fig. 2).
- e) The numerical analysis is evaluated for an ideal, perfectly plane plate

obeying the assumptions listed above. No account is taken of imperfections or strain hardening. The resulting solution will represent an upper bound on post-buckling behaviour of perfectly plastic plates.

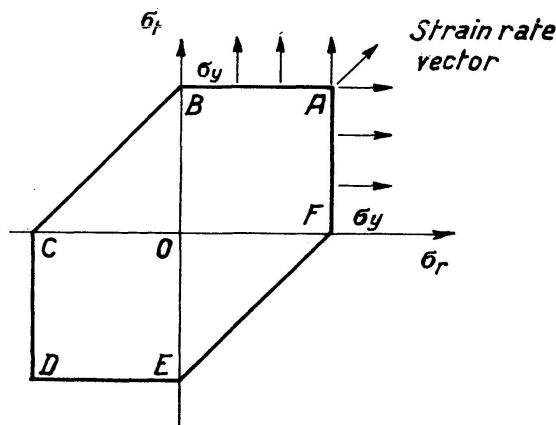


Fig. 2. The Tresca Yield Diagram.

### General Analysis

The loading path is evaluated for elastic behaviour throughout the plate but may be extended to include elastic-plastic behaviour by a suitable modification of the equations of moment, thrust and equilibrium. Solutions are derived for elastic, post-buckling behaviour involving simply supported and clamped plates; the solution for the plate with the elastically restrained edge may then be obtained by interpolating between the two limit solutions.

The moments and thrusts in the elastic plate may be derived with recourse to the system of strains and stresses in the plate at large deflexion:

$$\begin{aligned}
 m\epsilon_r &= \frac{du}{dr} + \frac{1}{2} \left( \frac{d\omega}{dr} \right)^2, & m\epsilon_t &= \frac{u}{r}, \\
 b\epsilon_r &= -z \frac{d^2\omega}{dr^2}, & b\epsilon_t &= -\frac{z}{r} \frac{d\omega}{dr}, \\
 m\sigma_r &= \frac{E}{1-\nu^2} \left[ \frac{du}{dr} + \frac{1}{2} \left( \frac{d\omega}{dr} \right)^2 + \nu \frac{u}{r} \right], & m\sigma_t &= \frac{E}{1-\nu^2} \left[ \frac{u}{r} + \nu \frac{du}{dr} + \frac{\nu}{2} \left( \frac{d\omega}{dr} \right)^2 \right], \\
 b\sigma_r &= -\frac{Ez}{1-\nu^2} \left[ \frac{d^2\omega}{dr^2} + \frac{\nu}{r} \frac{d\omega}{dr} \right], & b\sigma_t &= -\frac{Ez}{1-\nu^2} \left[ \frac{1}{r} \frac{d\omega}{dr} + \nu \frac{d^2\omega}{dr^2} \right], \\
 m_r &= -D \left[ \frac{d^2\omega}{dr^2} + \frac{\nu}{r} \frac{d\omega}{dr} \right], & m_t &= -D \left[ \frac{1}{r} \frac{d\omega}{dr} + \nu \frac{d^2\omega}{dr^2} \right].
 \end{aligned} \tag{1}$$

The subscripts  $r$  and  $t$  denote the radial and tangential directions respectively, subscript  $m$  denotes membrane effects and subscript  $b$  bending effects. The system of polar coordinates is referred to the centre of the plate.

The equations of equilibrium are obtained by considering the forces acting on a plate element shown in Fig. 3.

$$\frac{d^2 u}{dr^2} = -\frac{1}{r} \frac{du}{dr} + \frac{u}{r^2} - \frac{(1-\nu)}{2r} \left( \frac{d\omega}{dr} \right)^2 - \left( \frac{d\omega}{dr} \right) \left( \frac{d^2 \omega}{dr^2} \right), \quad (2)$$

$$\frac{d^3 \omega}{dr^3} = -\frac{1}{r} \frac{d^2 \omega}{dr^2} + \frac{1}{r^2} \frac{d\omega}{dr} + \frac{12}{h^2} \frac{d\omega}{dr} \left[ \frac{du}{dr} + \frac{1}{2} \left( \frac{d\omega}{dr} \right)^2 + \nu \frac{u}{r} \right]. \quad (3)$$

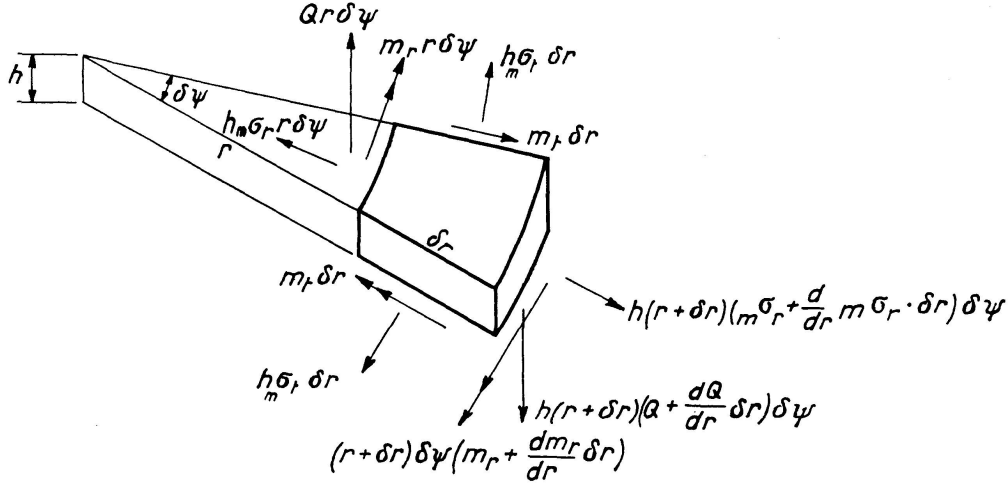


Fig. 3. Equilibrium of plate element.

Critical loads are obtained from Eq. (3) by recognizing the associated plane strain problem in the linear theory,

$$r^2 \frac{d^2 \varphi}{dr^2} + r \frac{d\varphi}{dr} + (q^2 r^2 - 1) \varphi = 0,$$

where  $\varphi = \frac{d\omega}{dr}$ ,  $q^2 = \frac{h p}{D}$ ,  $\nu = 0.3$  and  $-p = m \sigma_r$  is the applied edge compression.

The lowest resulting eigenvalues are given by:

$$p_{cr} = \frac{4.2 D}{h R^2} \quad \text{for the simply supported plate,}$$

$$p_{cr} = \frac{14.68 D}{h R^2} \quad \text{for the clamped plate.}$$

Post-buckling behaviour may be derived using a numerical method which uses the equations of equilibrium, moment and thrust. Introduce moment and thrust parameters  $\gamma$  and  $\beta$  such that

$$\gamma = \frac{m}{m_p}, \quad \beta = \frac{m \sigma}{\sigma_y}, \quad (4)$$

where  $m_p$  is the full plastic moment per unit width of plate  $\frac{h^2 \sigma_y}{4}$  and  $\sigma_y$  is the yield stress in simple tension or compression.

The initial conditions may be deduced by considering symmetry at the centre of the plate

$$\begin{aligned} u = \omega = 0, \quad \gamma_r = \gamma_t = \gamma_0, \quad \beta_r = \beta_t = \beta_0, \\ \frac{d\omega}{dr} = 0, \quad \frac{1}{r} \frac{d\omega}{dr} = \frac{d^2\omega}{dr^2}, \quad \frac{u}{r} = \frac{du}{dr}. \end{aligned} \quad (5)$$

Elastic behaviour in the plate is expressed as an interaction between moment and thrust.

$$\gamma \leq \frac{2}{3}(1 - |\beta|), \quad (6)$$

where  $|\beta|$  represents either tensile or compressive membrane stress in the plate. Elasticity at the centre of the plate does not necessarily imply elastic behaviour elsewhere, and further restrictions are required on the integration procedure insofar as combinations of moment and thrust must be investigated over each interval so as to retain elastic behaviour in the plate.

The system of equations representing elastic behaviour in the plate may be non-dimensionalised as follows:

$$\bar{\gamma} = \frac{\gamma}{k^2}, \quad \bar{\beta} = \frac{\beta}{k^2}, \quad \bar{\omega} = \frac{\omega}{h}, \quad \bar{u} = \frac{u}{h}, \quad \bar{r} = \frac{r}{h}, \quad k^2 = \frac{E}{3\sigma_y(1-\nu^2)},$$

when the relevant equations become:

a) equations of moment and thrust

$$\begin{aligned} \bar{\gamma}_r = - \left[ \frac{d^2\bar{\omega}}{d\bar{r}^2} + \frac{\nu}{\bar{r}} \frac{d\bar{\omega}}{d\bar{r}} \right], \quad \bar{\beta}_r = 3 \left[ \frac{d\bar{u}}{d\bar{r}} + \frac{1}{2} \left( \frac{d\bar{\omega}}{d\bar{r}} \right)^2 + \nu \frac{\bar{u}}{\bar{r}} \right], \\ \bar{\gamma}_t = - \left[ \frac{1}{\bar{r}} \frac{d\bar{\omega}}{d\bar{r}} + \nu \frac{d^2\bar{\omega}}{d\bar{r}^2} \right], \quad \bar{\beta}_t = 3 \left[ \frac{\bar{u}}{\bar{r}} + \nu \frac{d\bar{u}}{d\bar{r}} + \frac{1}{2} \left( \frac{d\bar{\omega}}{d\bar{r}} \right)^2 \right]. \end{aligned} \quad (7)$$

b) equations of equilibrium

$$\begin{aligned} \bar{r} \frac{d^2\bar{u}}{d\bar{r}^2} = - \frac{d\bar{u}}{d\bar{r}} + \frac{\bar{u}}{\bar{r}} - \frac{(1-\nu)}{2} \left( \frac{d\bar{\omega}}{d\bar{r}} \right)^2 - \bar{r} \left( \frac{d\bar{\omega}}{d\bar{r}} \right) \left( \frac{d^2\bar{\omega}}{d\bar{r}^2} \right), \\ \bar{r} \frac{d^3\bar{\omega}}{d\bar{r}^3} = - \frac{d^2\bar{\omega}}{d\bar{r}^2} + \frac{1}{\bar{r}} \frac{d\bar{\omega}}{d\bar{r}} + 12\bar{r} \left( \frac{d\bar{\omega}}{d\bar{r}} \right) \left[ \frac{d\bar{u}}{d\bar{r}} + \frac{1}{2} \left( \frac{d\bar{\omega}}{d\bar{r}} \right)^2 + \nu \frac{\bar{u}}{\bar{r}} \right]. \end{aligned} \quad (8)$$

c) initial conditions

$$\begin{aligned} \bar{u}_0 = \bar{\omega}_0 = 0, \quad \left( \frac{d\bar{\omega}}{d\bar{r}} \right)_0 = 0, \\ \left( \frac{d\bar{u}}{d\bar{r}} \right)_0 = \left( \frac{\bar{u}}{\bar{r}} \right)_0 = \frac{\bar{\beta}_0}{3(1+\nu)}, \quad \left( \frac{d^2\bar{\omega}}{d\bar{r}^2} \right)_0 = \left( \frac{1}{\bar{r}} \frac{d\bar{\omega}}{d\bar{r}} \right)_0 = - \frac{\bar{\gamma}_0}{(1+\nu)}, \\ \left( \bar{r} \frac{d^2\bar{u}}{d\bar{r}^2} \right)_0 = 0, \quad \left( \bar{r} \frac{d^3\bar{\omega}}{d\bar{r}^3} \right)_0 = 0. \end{aligned} \quad (9)$$

d) the test for elasticity

$$\text{at } \bar{r} = 0, \quad \bar{\gamma}_0 \leq \frac{2}{3} \left( \frac{1}{k^2} - |\bar{\beta}_0| \right), \quad (10)$$

$$\text{at } \bar{r}, \quad \bar{\gamma}_r \leq \frac{2}{3} \left( \frac{1}{k^2} - |\bar{\beta}_r| \right), \quad \bar{\gamma}_t \leq \frac{2}{3} \left( \frac{1}{k^2} - |\bar{\beta}_t| \right). \quad (11)$$

Before proposing a programme for the numerical integration of the differential equations of equilibrium, it is necessary to resolve the singularities in  $\frac{d^2 \bar{u}}{d \bar{r}^2}$  and  $\frac{d^3 \bar{\omega}}{d \bar{r}^3}$  which prevail at  $\bar{r} = 0$ . These singularities are of the form  $\frac{0}{0}$  which may be removed by using L'Hospital's Rule or referring the problem to new variables through the following identities,

$$\bar{\omega}(\bar{r}) = W(\bar{r}^2), \quad \bar{u}(\bar{r}) = \bar{r} U(\bar{r}^2), \quad \bar{r}^2 = x. \quad (12)$$

The transformed problem may be redefined in terms of new variables  $W, U, x$ :

a) equations of moment and thrust

$$\begin{aligned} \bar{\gamma}_r &= -[2(1+\nu)W' + 4xW''], & \bar{\beta}_r &= 3[(1+\nu)U + 2x(U' + W'^2)], \\ \bar{\gamma}_t &= -[2(1+\nu)W' + 4\nu xW''], & \bar{\beta}_t &= 3[(1+\nu)U + 2\nu x(U' + W'^2)], \end{aligned} \quad (13)$$

in which primes denote differentiation with respect to  $x$ .

b) equations of equilibrium

$$\begin{aligned} U'' &= -\frac{2}{x}U' + \frac{\nu-3}{2x}W'^2 - 2W'W'', \\ W''' &= -\frac{2}{x}W'' + \frac{3(1+\nu)}{x}UW' + 6W'(U' + W'^2). \end{aligned} \quad (14)$$

c) initial conditions

$$\begin{aligned} W_0 &= 0, & U_0 &= \frac{\bar{\beta}_0}{3(1+\nu)}, \\ W'_0 &= -\frac{\bar{\gamma}_0}{2(1+\nu)}, & U'_0 &= \frac{(\nu-3)\bar{\gamma}_0^2}{16(1+\nu)^2}, \\ W''_0 &= -\frac{\bar{\gamma}_0\bar{\beta}_0}{4(1+\nu)}, & U''_0 &= \frac{(\nu-5)\bar{\beta}_0\bar{\gamma}_0^2}{24(1+\nu)^2}, \\ W'''_0 &= \frac{\bar{\gamma}_0}{96(1+\nu)^2} [3(1-\nu)\bar{\gamma}_0^3 - 8(1+\nu)\bar{\beta}_0^2]. \end{aligned} \quad (15)$$

d) conditions for elasticity

$$\bar{\gamma}_0 \leq \frac{2}{3} \left( \frac{1}{k^2} - |\bar{\beta}_0| \right), \quad (16)$$

$$\bar{\gamma}_r \leq \frac{2}{3} \left( \frac{1}{k^2} - |\bar{\beta}_r| \right), \quad \bar{\gamma}_t \leq \frac{2}{3} \left( \frac{1}{k^2} - |\bar{\beta}_t| \right). \quad (17)$$

### Numerical Solution for Post-Buckling

The differential equations of equilibrium (14) may be integrated numerically using a fourth order Runge-Kutta process stored as a library subroutine in a digital computer. Before initiating the process, however, the equations must be conditioned such that each derivative is expressed explicitly as a function of the dependent variables. This is achieved by making the following substitutions:

$$x = s_1, \quad U' = s_2, \quad W' = s_3, \quad W'' = \frac{ds_3}{dx} = s_4.$$

The resulting set of simultaneous equations is of the form required in the subroutine

$$\begin{aligned} \frac{ds_2}{dx} &= F(s_1, s_2, s_3, s_4), & \frac{ds_4}{dx} &= G(s_1, U, s_2, s_3, s_4), \\ \frac{ds_1}{dx} &= 1, & \frac{ds_3}{dx} &= s_4, & \frac{dU}{dx} &= s_2. \end{aligned} \quad (18)$$

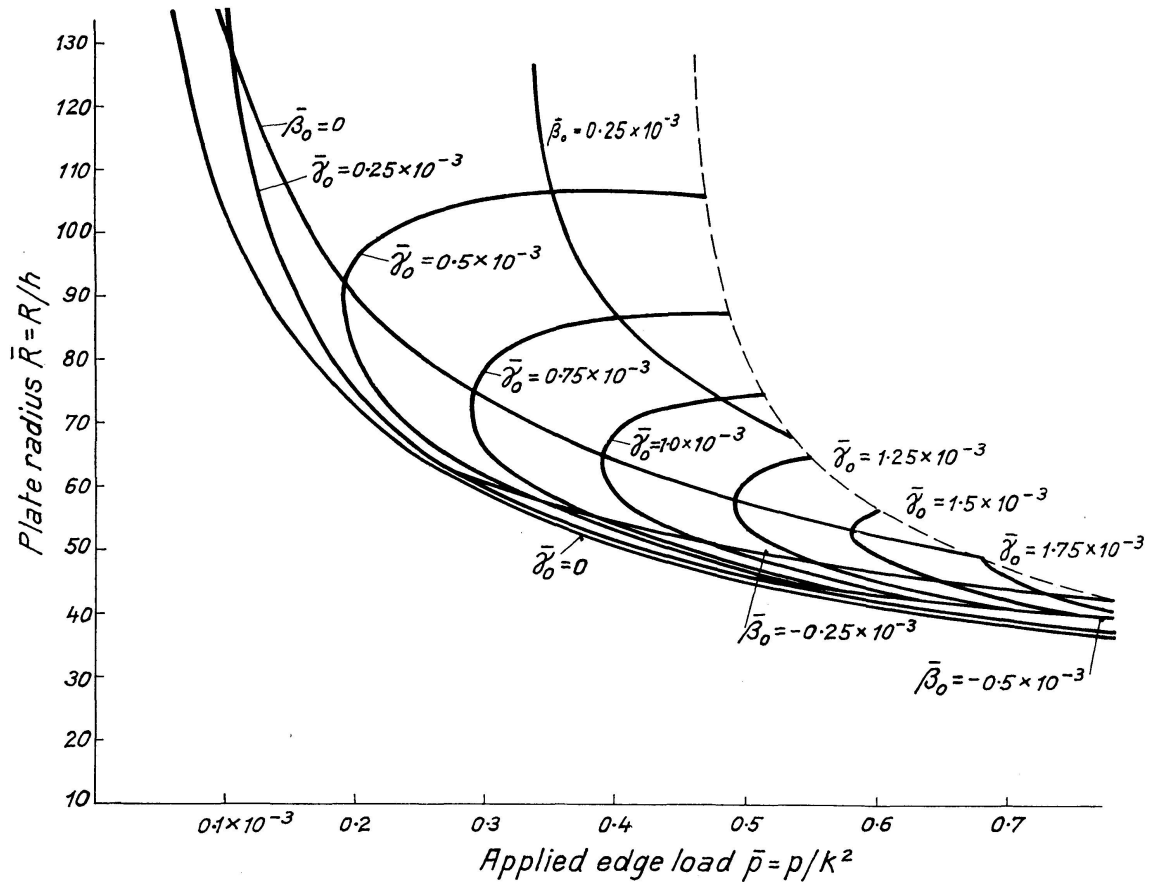


Fig. 4. Plate size vs. Edge load for the simply supported elastic plate.

The several stages of the programme are outlined thus:

- Stage 1:* Select values of  $\bar{\gamma}_0, \bar{\beta}_0$  in accordance with equation (16).  
*Stage 2:* Evaluate the initial conditions as given by equation (15).  
*Stage 3:* Advance the functions  $W, W', W'', W''', U, U', U''$  a single step  $\delta$  using the Runge-Kutta subroutine; evaluate the moments and thrusts as given by equation (13). Check the yield conditions, equation (17), to verify that elasticity is preserved at radius  $\delta$ .  
*Stage 4:* Repeat stage 3 until specified boundary conditions are attained. For the simple support obtain  $\bar{\gamma}_r = 0$ ; for the clamped edge obtain  $W' = 0$ .  
*Stage 5:* Print out results.

For the simply supported plate evaluate  
 the total radius  $\bar{R} = \sum \delta$

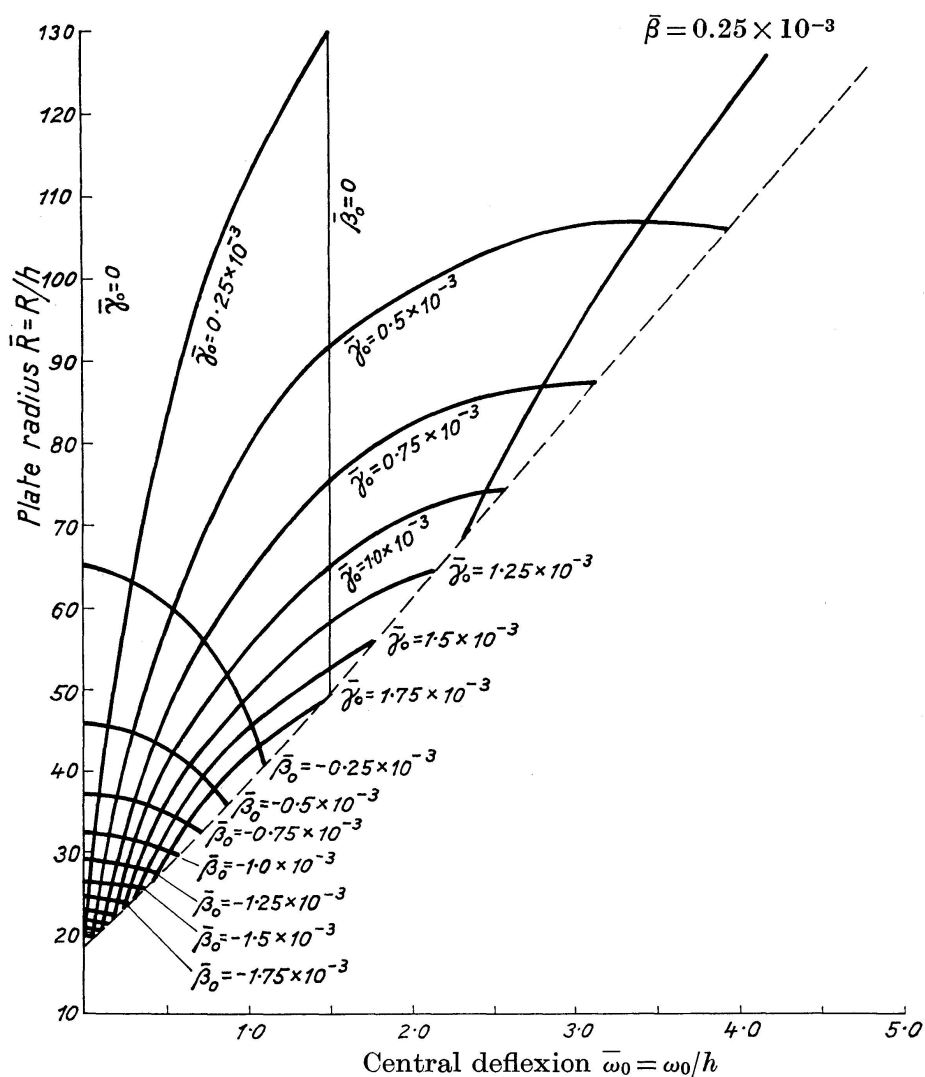


Fig. 5. Plate size vs. Central deflexion for the simply supported elastic plate.



the boundary thrust  $\bar{\beta}_R$   
the total central deflexion  $\bar{\omega}_0$

For the clamped plate obtain

the critical radius  $\bar{R} = \sum \delta$   
the boundary thrust  $\bar{\beta}_R$   
the boundary moment  $\bar{\gamma}_R$   
the total central deflexion  $\bar{\omega}_0$

*Stage 6:* Repeat stages 1 to 5 using different  $\bar{\gamma}_0, \bar{\beta}_0$ .

The programme was evaluated for several combinations of  $\bar{\gamma}_0$  and  $\bar{\beta}_0$ , positive  $\bar{\beta}_0$  being associated with a tension field and negative  $\bar{\beta}_0$  with a compressive field at the centre of the plate. The relationships between plate size, edge moment and thrust and central deflexion are given in *Figs. 4 to 8* through contours of moment and thrust acting at the centre. For a given plate size, the edge load and corresponding central deflexion are determined by reading off along a succession of contours. In deriving the results, a representative value of  $k^2 = 322$  was chosen for mild steel.

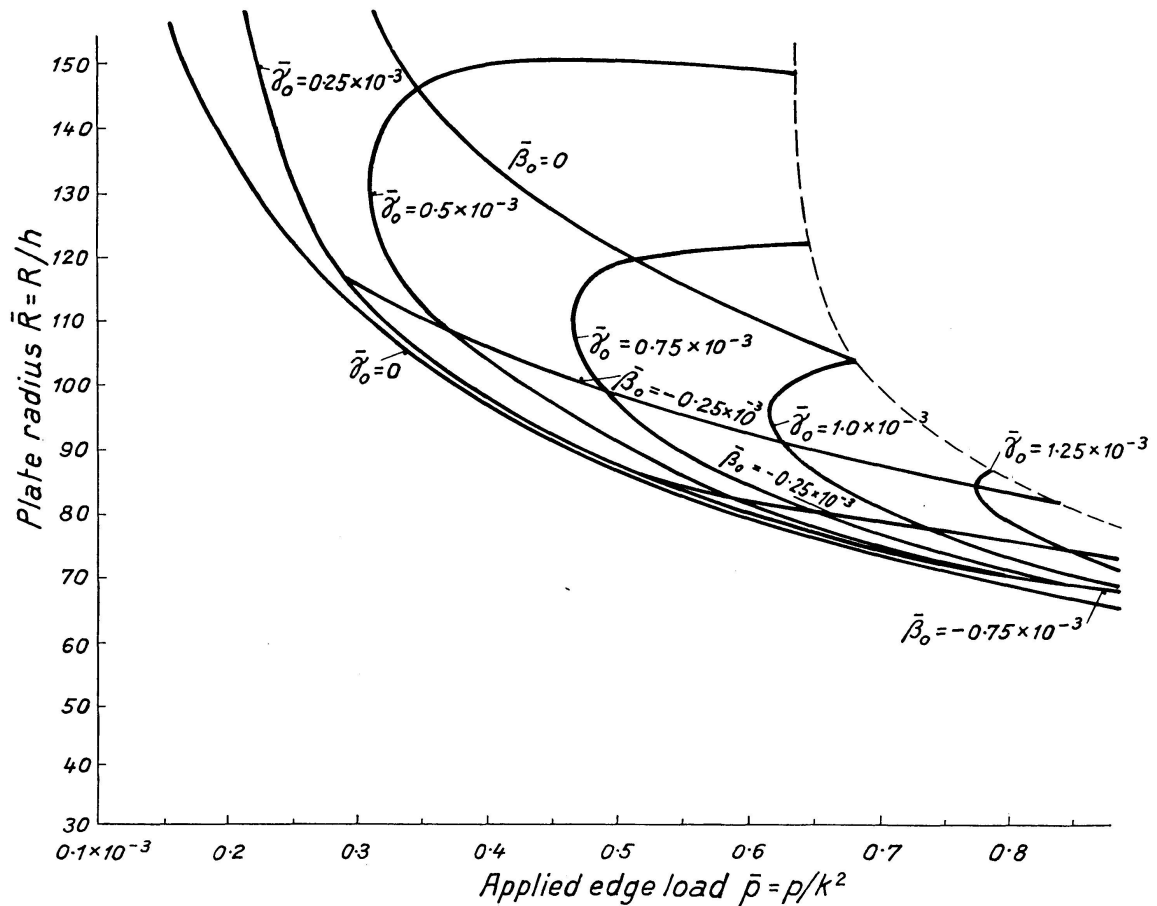


Fig. 6. Plate size vs. Edge load for the clamped elastic plate.

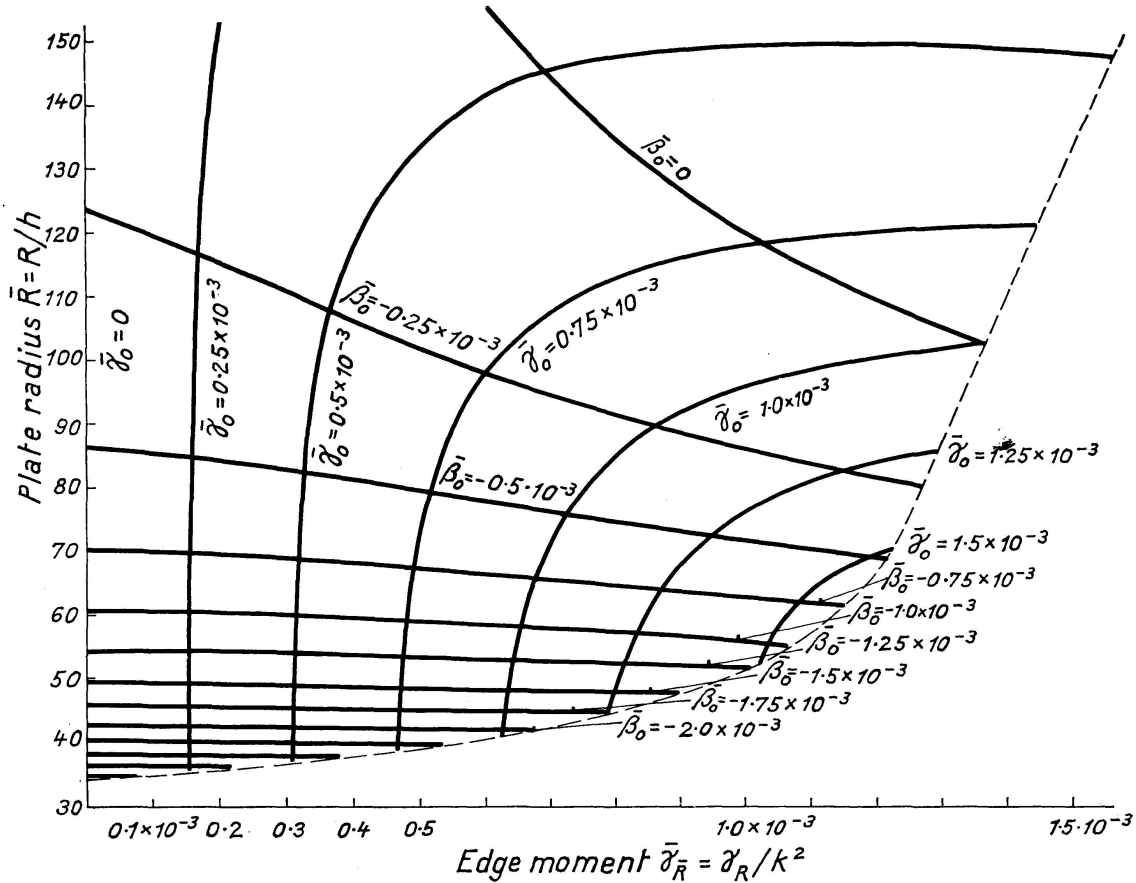


Fig. 7. Plate size vs. Edge moment for the clamped elastic plate.

### Mechanism Line for the Simply Supported Plate

An upper bound on the unloading of the circular plate in compression may be obtained by assuming an arbitrary hinge field and minimizing the applied edge load with respect to such a mechanism. The resulting collapse line is the locus of a succession of equilibrium problems showing the reduction in the rigid-plastic collapse load with changes in geometry of the plate.

The unloading line is derived using a rigid-perfectly plastic stress-strain law and a Tresca Yield criterion. As a consequence of these assumptions, points within the yield diagram are assumed to remain rigid, and a mechanism may be postulated in which all radial plastic flow is concentrated in a hinge circle corresponding to the sides  $AF$  and  $CD$  of the yield hexagon and tangential yielding takes place within a set of  $2\pi$  hinge lines associated with the sides  $AB$  and  $DE$  of the diagram.

A general mechanism of deformation for the simply supported plate is shown in Fig. 9. The mechanism consists of a hinge circle circumscribing a rigid central core of radius  $\mu R$  and a set of hinge lines  $1 > y > \mu$  such that  $y$  is a non-dimensional radius defining a general annulus in the plate,  $\alpha$  a non-

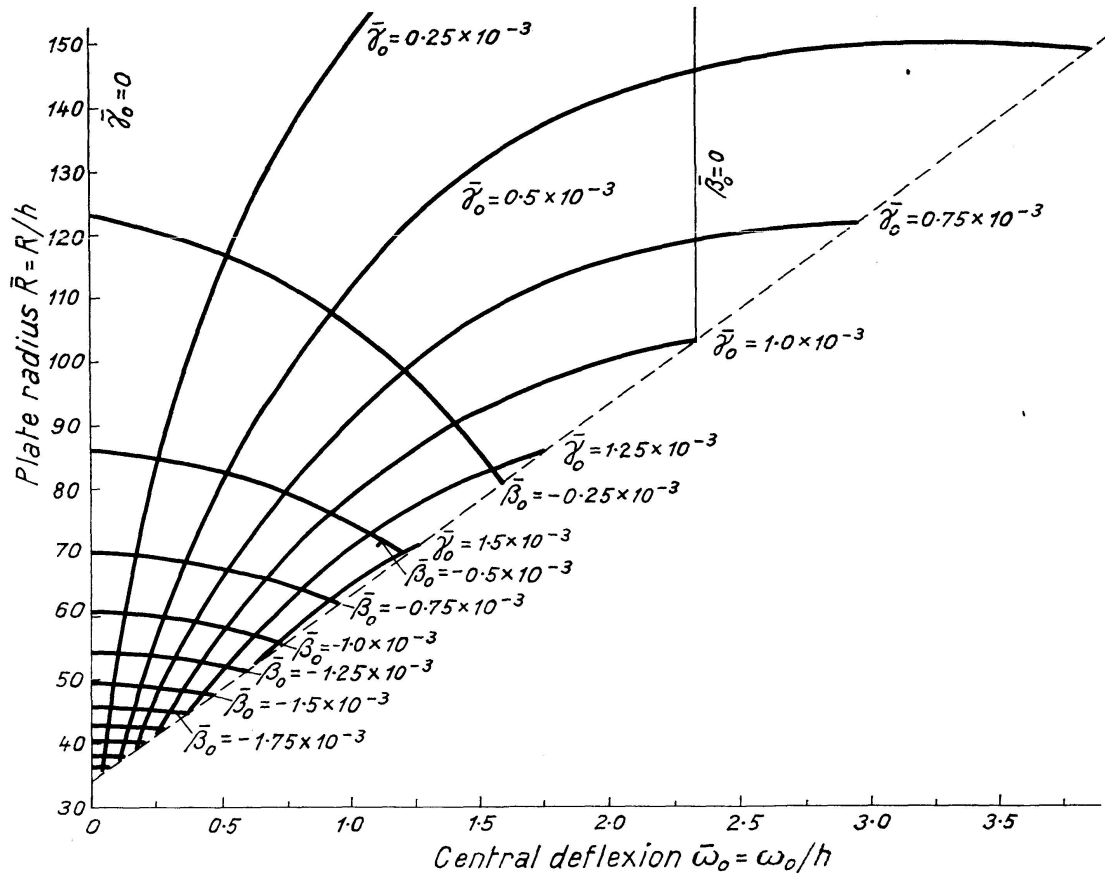


Fig. 8. Plate size vs. Central deflexion for the clamped elastic plate.

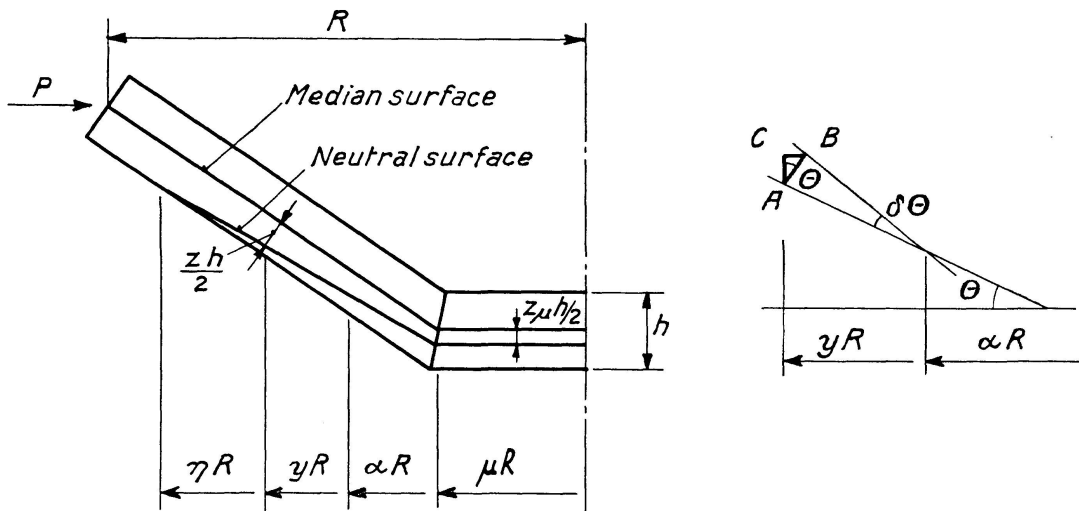


Fig. 9. A general mechanism for the simply supported circular plate in compression.

dimensional radius at which the tangential strain is zero, and  $\eta$  a non-dimensional radius defining the limiting neutral surface in the bent plate. The distance between the neutral and median surfaces is given by

$$z = 2 \left( \frac{R \theta}{h} \right) (y - \alpha).$$

The neutral surface is defined by considering the limits  $z = z_\mu$  for  $y = \mu$  and  $z = 1$  for  $y = \eta$ ,

$$z_\mu = 2 \left( \frac{R \theta}{h} \right) (\mu - \alpha), \quad \eta = \alpha + \frac{h}{2 R \theta}. \quad (19)$$

The applied load  $p$  is determined by considering equilibrium across a radius  $R$ .

$$p R = \int_{\mu}^{\eta} z \sigma_y h R dy + \int_{\eta}^1 \sigma_y h R dy + \mu R h z_\mu \sigma_y.$$

Integrating the right hand side yields the required relationship,

$$p = h \sigma_y \left[ 1 - \alpha - \frac{h}{4 R \theta} + \frac{R \theta}{h} (\mu^2 - \alpha^2) \right]. \quad (20)$$

The load  $p$  may be minimised with respect to the assumed hinge field

$$\frac{dp}{d\mu} = 0 = -\frac{d\alpha}{d\mu} + 2 \left( \frac{R \theta}{h} \right) \left( \mu - \alpha \frac{d\alpha}{d\mu} \right),$$

$$\text{from which} \quad \frac{d\alpha}{d\mu} = \frac{2 \mu \left( \frac{R \theta}{h} \right)}{1 + 2 \alpha \left( \frac{R \theta}{h} \right)}. \quad (21)$$

$\mu$  and  $\alpha$  may be determined from the work done in the bent plate. For a virtual displacement  $\delta \theta$  about an equilibrium position  $\theta$ , the total internal work  $U_i$  is given by the work done in the hinge lines  $1 \geq y \geq \mu$  and the hinge circle  $\mu R$ .

$$\frac{U_i}{2 \pi R h^2 \sigma_y \delta \theta} = \frac{h}{24 R \theta} + \frac{\alpha}{4} + \frac{R \theta}{h} \frac{(1 - \alpha)^2}{2} + \left( \frac{R \theta}{h} \right)^2 \frac{(\mu - \alpha)^2}{3} (2 \mu + \alpha).$$

The external work  $U_e$  is the work done by the applied load  $p$

$$U_e = 2 \pi R h \delta \theta \left( \frac{R \theta}{h} \right) (1 - \alpha) h \sigma_y \left[ 1 - \alpha - \frac{h}{4 R \theta} + \left( \frac{R \theta}{h} \right) (\mu^2 - \alpha^2) \right]$$

By the Principle of Virtual Work  $U_i = U_e$  or

$$\frac{h}{24 R \theta} + \frac{1}{4} - \left( \frac{R \theta}{h} \right) \frac{(1 - \alpha)^2}{2} + \frac{1}{3} \left( \frac{R \theta}{h} \right)^2 [(2 \mu + \alpha) (\mu - \alpha)^2 - 3 (1 - \alpha) (\mu^2 - \alpha^2)] = 0. \quad (22)$$

The parameter  $\alpha$  may also be minimised with respect to the assumed hinge field  $\mu$  to yield

$$\frac{d\alpha}{d\mu} = - \frac{2 \left( \frac{R \theta}{h} \right) \mu (\mu - 1)}{(1 - \alpha) \left[ 1 + 2 \alpha \left( \frac{R \theta}{h} \right) \right]}. \quad (23)$$

Comparing Eqs. (21) and (23)

$$\mu = \alpha. \quad (24)$$

From this relationship it follows that the general mechanism of deformation is possible only when the neutral and median surfaces coincide for  $y \leq \mu$  i.e.  $z_\mu = 0$ . Inserting  $\mu = \alpha$  in Eq. (22) and regarding  $\frac{R\theta}{h}$  as a non-dimensional deflexion  $\Delta$  obtain

$$12(1-\mu)^2 \Delta^2 - 6\Delta - 1 = 0.$$

The case  $\mu = 0$  occurs when

$$12\Delta^2 - 6\Delta - 1 = 0$$

or

$$\Delta = \Delta' = 0.631. \quad (25)$$

The corresponding value of  $p$  may be obtained from Eq. (20)

$$\frac{p}{h\sigma_y} = 0.604. \quad (26)$$

The behaviour of the plate may be described in three well defined stages shown in Fig. 10; the load-deflexion relationships corresponding to each stage

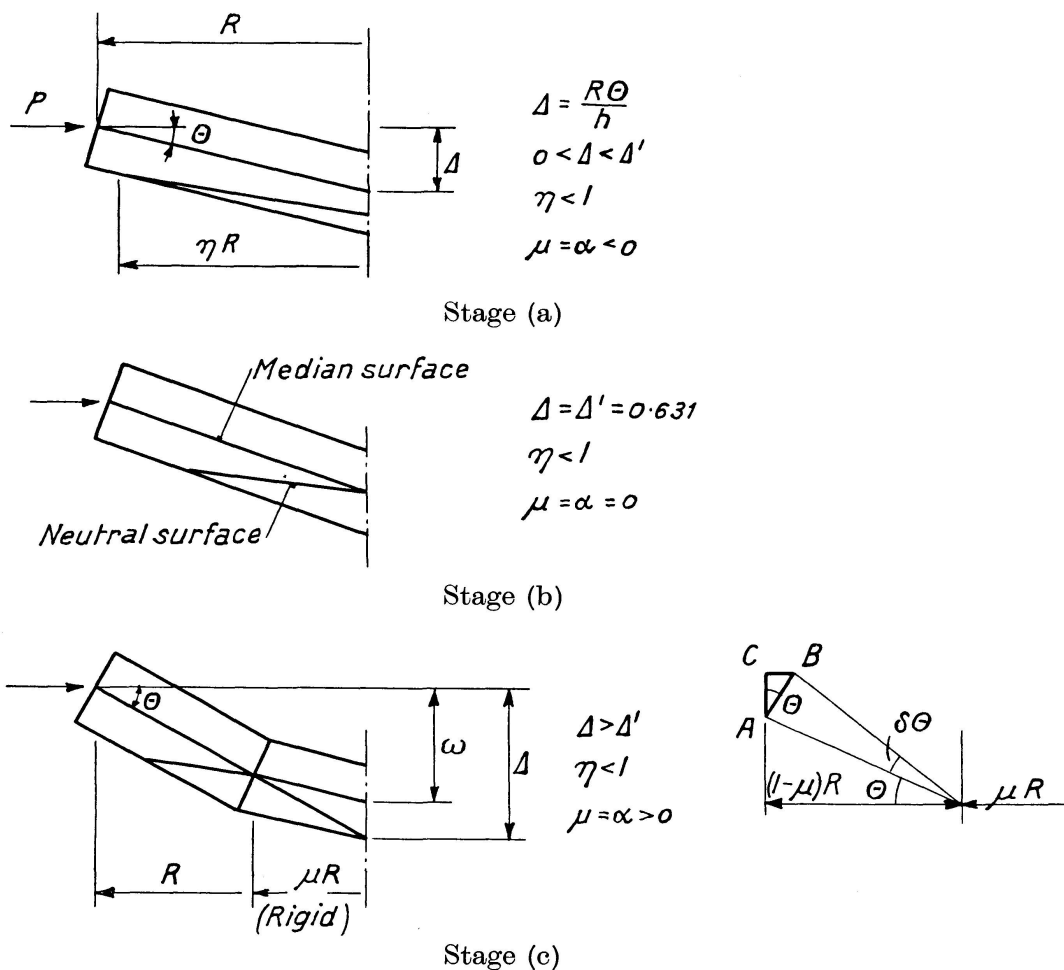


Fig. 10. Unloading of a rigid-plastic, simply supported circular plate.

are as follows:

Stage (a) is relevant for  $0 \leq \Delta < \Delta'$ ; the load and deflexion may be expressed as functions of  $\alpha$ .

$$\begin{aligned} \frac{p}{h \sigma_y} &= 1 - \alpha - \frac{1}{4\Delta} - \Delta \alpha^2, \\ 8\alpha^2(3 - 2\alpha)\Delta^3 - 12(1 - \alpha)^2\Delta^2 + 6\Delta + 1 &= 0. \end{aligned} \quad (27)$$

The necessary restrictions on this range are given by:

$$\gamma = \alpha + \frac{1}{2\Delta} < 1, \quad \mu = \alpha < 0.$$

Stage (b) is a single point on the load-deflexion curve

$$\frac{p}{h \sigma_y} = 0.604, \quad \Delta = 0.631 \quad (28)$$

and the necessary conditions for the existence of such a point are

$$\mu = \alpha = 0, \quad \gamma < 1.$$

These restrictions imply that the centre of the plate is under pure plastic moment.

Stage (c) where the hinge circle which develops at the centre of the plate in the previous stage begins to move radially outward; the restrictions on this stage are that

$$\mu = \alpha > 0, \quad \gamma < 1.$$

The relevant parametric equations defining this stage are specified in terms of  $\mu$ .

$$\frac{p}{h \sigma_y} = 1 - \mu - \frac{1}{4\Delta}, \quad 12(1 - \mu)^2\Delta^2 - 6\Delta - 1 = 0. \quad (29)$$

It should be noted that  $\Delta$  no longer represents the central deflexion of the plate; its relation to the true deflexion  $w$  is seen in Fig. 10c. For  $\Delta > \Delta'$  the total deflexion becomes

$$\frac{w}{h} = \Delta' + \int_{\Delta'}^{\Delta} (1 - \mu) d\Delta.$$

It is possible to transform the equations for this stage of unloading into a pair of parametric equations in  $\Delta$  instead of  $\mu$ .

$$\begin{aligned} \frac{p}{h \sigma_y} &= \frac{1}{4\Delta} [2\sqrt{2\Delta + \frac{1}{3}} - 1], \\ \frac{w}{h} &= -0.631 + \sqrt{2\Delta + \frac{1}{3}} + \frac{1}{2\sqrt{3}} \log_e 2.68 \left[ \frac{\sqrt{6\Delta + 1} - 1}{\sqrt{6\Delta + 1} + 1} \right]. \end{aligned} \quad (30)$$

The non-dimensional mechanism line for the three stages of unloading is plotted in Fig. 11, the curve being a synthesis of Eqs. (27), (28) and (30).

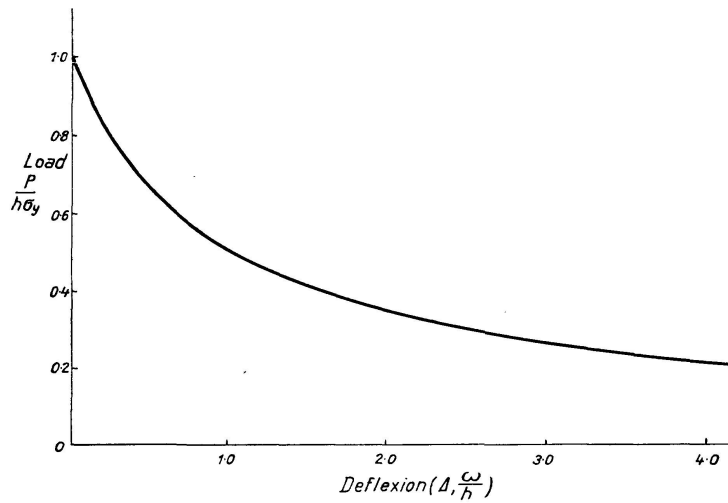


Fig. 11. The mechanism line for a rigid-plastic, simply supported circular plate in compression.

### Conclusions

The analyses for the loading and unloading paths are developed on the basis of a symmetrical fundamental buckling mode for circular plates and will thus be restricted to that class of moderately thick plates for which such a mode can be realized. For very thin plates the analyses may be completely inaccurate owing to asymmetrical buckling modes which result from high tangential stresses occasioned in the perimeter of plate at finite deflexions. In such problems the mechanism of plastic flow is considerably more complex than the simple pattern proposed here. Furthermore the solutions are applicable only to those plates which possess no imperfections and exhibit no work hardening and, as such, estimates of the collapse load will represent upper bounds on the correct failure loads. It was mentioned earlier that the discrepancy between points *C* and *X* in Fig. 1 arose from a fundamental difference in the stress-strain laws governing the loading and unloading paths, the former being derived for an elastic-plastic material and the latter for a rigid-plastic material. It may be pointed out that the range *BC* of the loading path represents an increasing flexibility of the plate resulting from a deterioration of the elastic stiffness due to the incidence of localised plastic flow; an estimate of the ultimate load capacity may therefore be made by extending the elastic loading path to intersect the plastic unloading line in point *Y* (Fig. 1) lying above *X*. For thin plates the difference in ultimate loads between points *X*, *Y* and *C* will be considerable, but for moderately thick plates this

difference becomes less critical until, for plates which buckle at the yield stress, the three points are combined into a single yield load, representative of the ultimate strength. From the foregoing analysis it should be possible to estimate the ultimate strength of simply supported circular plates.

A general load-deflexion relationship for the elastic, post-buckling behaviour of circular plates in compression may be derived from the contours of Figs. 4 to 8. Such a relationship is of the form

$$\frac{P}{P_y} = -k_1 \left( \frac{E}{\sigma_y} \right) \left( \frac{h}{R} \right)^2 - k_2 \left( \frac{E}{\sigma_y} \right) \left( \frac{h}{R} \right)^2 \left( \frac{\omega_0}{h} \right)^2, \quad (31)$$

in which the first term on the right hand side represents the critical thrust and the second term parabolic, post-buckling behaviour. Eq. (31) may be fitted to the contours obtained from the computer programme by plotting the load versus the square of the deflexion for plates of various sizes. The locus of all points, for a given plate size  $R/h$ , will constitute a straight line intersecting the load axis in the critical load and having a slope defining the coefficient of  $\left( \frac{\omega_0}{h} \right)^2$ . The coefficients then become:

For the simply supported plate  $k_1 = 0.385$ ,  $k_2 = 0.093$ .

For the clamped plate  $k_1 = 1.348$ ,  $k_2 = 0.22$ .

A curious feature of the mechanism line is its analogy to the "effective width" concept obtaining in elastic plates. In the latter problem, the hypothesis suggests that, in post-buckling, a major part of the applied load is resisted by an edge strip of the plate. In the plastic problem, on the other hand, a similar concept becomes apparent only at deflexions  $\Delta > 0.631$ . In this range, the hinge circle, which first forms at the center, travels outward and an increasing core of the plate remains rigid. An inspection of the equations of equilibrium shows that the applied edge thrust is being resisted by tangential membrane forces across an edge strip of decreasing width. The movement of the hinge circle continues until the central rigid zone of the plate, surrounded by a plastic annulus, becomes too large to remain stable.

### Acknowledgements

The work described in this paper was carried out under the general direction of Professor J. F. Baker in the Engineering Laboratories of the University of Cambridge. The results obtained on EDSAC are published with the permission of the Director of the Cambridge University Mathematical Laboratory. Miss. G. M. Christ programmed the problem.



### Appendix

The equation of the load-deflexion curve in the vicinity of the critical load may be determined from the total elastic energy of the bent plate.

$$V = V_B + V_M + V_N, \quad (a)$$

where the subscripts  $B$  and  $M$  denote bending and membrane components of the internal strain energy and  $V_N$  is the external work done by the applied loads.

At large deflexion the total energy may be expressed in terms of the load  $P$  and the radial and transverse displacements  $u$  and  $w$  respectively.

$$V = f_1(\omega^2) + f_2(u^2, u\omega^2, \omega^4) + f_3(Pu). \quad (b)$$

The Theorem of Minimum Potential Energy stipulates that

$$\frac{\partial V}{\partial \omega} = 0, \quad (c)$$

$$\frac{\partial V}{\partial u} = 0. \quad (d)$$

From (c), it is possible to obtain  $u$  as a function of  $w$

$$u = f_4(\omega^2). \quad (e)$$

Applying condition (d) and inserting the relationship (e) obtain

$$0 = f_5(\omega) + f_6(\omega^3) + f_7(P\omega). \quad (f)$$

The resulting relationship is of the form:

$$P = P_{cr} + K\omega^2. \quad (g)$$

### References

- BODNER, S. R., 1954: The Post-Buckling Behaviour of a Clamped Circular Plate. *Quart. App. Math.*, Vol. 12, p. 397.
- FRIEDRICHS, K. O., STOKER, J. J., 1942: Buckling of a Circular Plate beyond the Critical Thrust. *J. App. Mech.* Vol. 9, p. A7.
- HOFF, N. J., 1949: Dynamic Criteria of Buckling. *Proc. Colston Res. Soc.*, Butterworths Scientific Pubn., London, p. 121.
- HORNE, M. R., 1956: The Elastic-Plastic Theory of Compression Members. *J. Mech. Phys. Solids*, Vol. 4, p. 104.
- HORNE, M. R., 1961: The Stability of Elastic-Plastic Structures. *Progress in Solid Mechanics*, Vol. 2, North Holland Pubn. Co., Amsterdam, p. 279.
- KELLER, H. B., REISS, E. L., 1958: Non-linear Bending and Buckling of Circular Plates. *Inst. of Math. Sc.*, New York Univ.
- TIMOSHENKO, S., 1940: *Theory of Plates and Shells*. McGraw Hill Book Co. Inc., New York, pp. 329, 333.
- WAY, S., 1934: Bending of Circular Plates with Large Deflexions. *Trans. ASME*, Vol. 56, p. 627.

### Summary

The ultimate strength of a simply supported circular plate in uniform compression is determined from the intersection of a loading path and a mechanism line. The former is shown to occur subsequent to buckling and a load-deflexion relationship is derived using a numerical method in conjunction with equations of equilibrium, moment and thrust. The resulting solution is extended to include the clamped circular plate. The mechanism line is determined by minimising the applied edge load with respect to an admissible hinge field in the plate at finite deflexion. The resulting load-deflexion curve represents the variation of collapse load with changes in geometry and may be regarded as the locus of a succession of equilibrium problems.

An estimate of the ultimate load is obtained by considering an elastic loading path and a rigid-plastic mechanism line. The resulting collapse load, known to provide an upper bound, is discussed in relation to the true collapse load.

### Résumé

La résistance limite d'une plaque circulaire simplement appuyée, soumise à des efforts de compression uniformes, est déterminée par l'intersection d'une courbe de charge et d'une courbe donnée par le calcul plastique (mécanisme). La première décrit le comportement post-critique de la plaque voilée; par une méthode numérique employée conjointement avec les équations d'équilibre, les équations des moments et celles des efforts du plan moyen, on déduit une relation charge/déformation. La solution obtenue est étendue aux plaques circulaires encastrées. La courbe du mécanisme est déterminée en calculant la valeur minimum de la charge appliquée correspondant à une configuration admissible des rotules plastiques dans la plaque, pour des déformations finies. La courbe charge/déformation obtenue représente les variations de la charge de ruine en fonction des modifications géométriques et peut être considérée comme le lieu géométrique d'une série de problèmes d'équilibre.

Une estimation de la charge limite est obtenue en considérant une courbe de charge élastique et une courbe de mécanisme plastique-rigide. La charge de ruine obtenue, qui constitue une limite supérieure, est discutée en relation à la charge de ruine réelle.

### Zusammenfassung

Die Grenzfestigkeit einer freidrehbar gelagerten Kreisplatte unter gleichförmigem Druck wird nach dem Schnittpunkt einer Belastungskurve und einer Mechanismuslinie bestimmt. Es wird gezeigt, daß die erstere nach dem Aus-

beulen erfolgt; unter Anwendung einer numerischen Methode im Verein mit Gleichgewichts-, Moment- und Längskraftgleichungen wird eine Last-Durchbiegungs-Beziehung abgeleitet. Die erhaltene Lösung wird auf die eingespannte Kreisplatte erweitert. Die Mechanismuslinie wird durch Berechnung der minimalen, am Rand wirkenden Belastung bezogen auf eine zulässige Gestaltung der plastischen Gelenke in der Platte bei endlicher Durchbiegung bestimmt. Die erhaltene Last-Durchbiegungs-Kurve stellt die Veränderung der Traglast mit den Änderungen in der Geometrie dar und kann als geometrischer Ort einer Reihe von Gleichgewichtsproblemen betrachtet werden.

Man gelangt zu einem Näherungswert für die Grenzlast durch Berücksichtigung einer elastischen Belastungskurve und einer starr-plastischen Mechanismuslinie. Die sich ergebende, einen oberen Grenzwert darstellende Traglast wird im Zusammenhang mit der effektiven Traglast besprochen.